Research highlights:

- Freshly emitted nanoparticles were found in the car cabin
- High frequency measurements are needed for better PNC estimation
- Dilution was found to be the dominant process in car cabin
- PNC levels in car cabin increased significantly in traffic congestion zones
- Exposure doses to temporal PNC peaks were up to 380% more than average dose rate.

Citation details:
Joodatnia, P., Kumar, P., Robins, A., 2013. The behaviour of traffic produced nanoparticles in a car cabin and resulting exposure rates. Atmospheric Environment 65, 40-51.

The behaviour of traffic produced nanoparticles in a car cabin and resulting exposure rates

Pouyan Joodatnia [a], Prashant Kumar [a, b, *], Alan Robins [b]

[a] *Department of Civil and Environmental Engineering, Faculty of Engineering and Physical Science (FEPS), University of Surrey, GU2 7XH, United Kingdom*

[b] *Environmental Flow (EnFlo) Research Centre, FEPS, University of Surrey, GU2 7XH, United Kingdom*

Abstract

The aim of this study is to assess particle number concentrations (PNCs) and distributions (PNDs) in a car cabin while driving. Further objectives include the determination of the influence of particle transformation processes on PNCs, PNDs and estimation of PNC related exposure. On–board measurements of PNCs and PNDs were made in the 5–560 nm size range using a fast response differential mobility spectrometer (DMS50), which has a response time of 500ms. Video records of the traffic ahead of the experimental car were also used to correlate emission events with measured PNCs and PNDs. A total of 30 return trips was made on a 2.7 kilometres route during morning and evening rush hours, with journey times of 7±2 and 10±3 minutes, respectively. The average PNC for the set of morning journeys, $5.79\pm3.52\times10^{4}$ cm^{-3}, was found to be nearly identical to the average recorded during the afternoon, $5.95\pm4.67\times10^{4}$ cm^{-3}. Average PNCs for individual trips varied from 2.42×10^{4} cm^{-3} to 2.18×10^{5} cm^{-3}, mainly due to changes in the emissions affecting the experimental car (e.g. when the experimental car was following another vehicle). The largest one second averaged PNC during a specific event, 1.85×10^{6} cm^{-3}, was found to be over 30–times greater than the overall–average of $5.87\pm4.06\times10^{4}$ cm^{-3}. Correlation of video records and concentration data indicated that close proximity to a preceding vehicle led to a clear increase in PNCs of freshly emitted nucleation mode particles. The evolution of normalised PNDs demonstrated that dilution was the dominant transformation process in the car cabin. The deposition of inhaled particles in the lung was estimated on the basis of either the size–resolved distribution or the total PNC. In general, the two methods yielded similar results but differences up to 30% were noted in some cases, with the latter method giving the lower values. Overall, the results reflect the importance of size–resolved measurements for deriving accurate evaluations of exposure rates, as well as identifying emissions from nearby traffic as the cause of short term elevations of PNCs and hence dose rates.

Keywords: Car cabin exposure; Nanoparticles dispersion; Number and size distribution; Ultrafine particles; Vehicle emissions

[*] Corresponding author. Department of Civil and Environmental Engineering (C5), Faculty of Engineering and Physical Sciences, University of Surrey, Guildford GU2 7XH, UK. Tel.: +44 1483 682762; fax: +44 1483 682135. E-mail addresses: P.Kumar@surrey.ac.uk; Prashant.Kumar@cantab.net

1. Introduction

Emissions from conventional fuel driven vehicles are generally the dominant contributor to particle number concentrations (PNCs) in the urban atmosphere (Kumar et al., 2010). The adverse impacts of nanoparticles (taken here to be those below 300 nm in diameter) on human health and the environment have raised concerns and attracted the attention of both the research community and policy makers (Atkinson et al., 2010; Kumar et al., 2011a). Recent studies have shown that commuters are likely to experience elevated exposure to airborne particulate matter (PM) while travelling by taxis, buses and trains within urban areas (Knibbs et al., 2011). Dons et al., (2011) indicate that personal exposure is significantly correlated to activity patterns of individuals. Even brief exposure to peaks of traffic related air pollution can elicit physiological changes that are consistent with the long term effects seen in epidemiological studies (Peter et al., 2004). The work of Dons et al. (2012) shows that ~6% of daily time spent in transport microenvironments can contribute to ~21% of total daily exposure. Concentrations of particulate material are expressed in either a mass or number form, though only PNCs and related particle number distributions (PNDs) are considered in this study. Nanoparticles dominate PNCs in urban areas but have negligible mass in comparison with larger sized particles such as PM_{10} and $PM_{2.5}$ (i.e. those below 10 and 2.5 μm in diameter, respectively) (Buseck and Adachi, 2008; Seinfeld and Pandis, 2006). Compared with coarse particles, nanoparticles provide a larger total surface area for the absorption of harmful organic chemicals and penetrate deeper into the lungs (Donaldson et al., 2005; Oberdorster, 2000). It is widely accepted that traffic related nanoparticles are main driving factor for short or long term health issues, such as neurological effects and cardiovascular diseases (Dons et al., 2012; Bos et al., 2011). Considering only mass metrics for air quality monitoring studies can clearly misrepresent the importance of nanoparticle numbers, which should perhaps be considered along with PM_{10} and $PM_{2.5}$ (Ghio et al., 2000; Wichmann and Peters, 2000) in defining air quality. An adequate understanding of PNCs during typical road journeys, especially during periods of high concentrations that might be up to two orders of magnitude above the long–term averaged (Kumar et al., 2008a), is essential in order to assess exposure related health risks (Knibbs and de Dear, 2010).

Reported exposure studies have generally used relatively long–term (i.e. monthly/daily) averaged concentration data from fixed-site monitoring stations alongside busy streets to characterise concentrations and public exposure levels (Knibbs and de Dear, 2010; Wang and Gao, 2011). Further, Dons et al. (2011) found that exposure estimated during transport is up

to 30% greater than those estimated at the fixed locations (e.g. residential). For instance, Wang and Gao (2011) reported that real–time PNC measurements at a relatively high sampling frequency (i.e. 1 Hz) can be 20–200% greater than historical (i.e. monthly-averaged) data obtained from fixed-site measurements. Little can be learnt of any transformation processes that occur on very short time scales (e.g. much smaller than 1 second) or realistic short–term personal exposure rates from the latter source. von Klot et al. (2011) show that exposure assessments based on background PNCs tend to underestimate and poorly predict the inhaled doses and personal exposure. This indicate the need of high frequency, real-time data from locations near to the main sources are required as well as taking into account activity pattern and time spent in transport microenvironments (von Klot et al., 2011; Dons et al., 2011). Therefore, nanoparticle concentration measurements with fast response instrumentation are essential to understand particle dispersion and dynamics, and for the accurate quantification of personal exposure.

Instruments commonly used for PNC measurements are summarised in Table 1. Rapid technological advances over the past few years have made available fast response (e.g. 200 ms) measurement systems; for further details, see the review of instruments in Kumar et al. (2010). Some studies have attempted to correlate temporal variations of PNCs with real-time emissions from traffic (Boogaard et al., 2009; Gouriou et al., 2004; Kaur et al., 2006). However, no previous effort has been made to correlate size–resolved particle behaviour within a car cabin to traffic events, especially during events that lead to considerably elevated concentration levels in the cabin.

Knibbs et al. (2011) recently reviewed a number of studies addressing the exposure of commuters in transport micro-environments. In general, car commuters experienced greater PNCs compared with those using other modes of transport, such as buses, ferries or cycles (Int Panis et al., 2010; Wang and Gao, 2011; Dons et al., 2012). Similar findings were reported by Kaur et al. (2005) in London, where car drivers were found to be exposed to somewhat greater PNC levels than pedestrians. In general, users of road transport (i.e. buses and cars) are likely to experience greater PNC exposure than those using other modes of transport (i.e. ferries and trains) (Knibbs and de Dear, 2010). This observation suggests that particle transformation rates and dynamics may vary between the modes of transport because of the different ranges of PNCs encountered (Kumar et al., 2010; Morawska et al., 2008).

Factors responsible for large temporal variations in PNCs within road transport vehicles include traffic conditions (e.g. composition, number and congestion), vehicle ventilation characteristics and meteorological conditions. For example, Zhu et al. (2007) concluded that well-functioning cabin filtration systems were much more effective against coarse particles than nanoparticles, probably because nanoparticles are smaller than the filter texture. The type of ventilation (mechanical or natural) can also influence PNCs, resulting in lower concentrations in vehicles with mechanically operated ventilation systems in comparison with those with natural ventilation, (Knibbs and de Dear, 2010; Rim et al., 2008). Fruin et al. (2011) suggest that the ventilation settings and subsequently air exchange rate ( ) has significant influence on flux rate of PNCs into the car cabin. General consensus is that increases when windows are kept open compared to other ventilation settings, such as recirculation fan setting (Fruin et al., 2011; Hudda et al., 2012). Further, Fruin et al. (2011) show that the increases at higher travelling speeds under recirculation fan setting. The present work was designed to overcome the limitations of the low frequency and relatively long–term averaged measurements of previous studies. A fast response differential mobility spectrometer (Cambustion DMS50, with a response time of 500ms) was deployed to measure the number and size distributions of particles in the cabin of a car. Videos of the traffic ahead of the car were also recorded to help identify the sources responsible for enhanced concentration levels and to correlate particle dynamics and exposure associated with the road traffic conditions.

2. Methodology

2.1. Study design and route characteristics

Measurements were made during car journeys in Guildford, a typical UK town that has 129,700 inhabitants (Census 2001). Car ownership in Guildford Borough is greater than the national level with, on average, each household possessing more than two cars (Guildford-Borough, 2008). Thirty experimental journeys (hereafter denoted as J_x, with the subscript indicating the journey number) were completed, during which PNC measurements were made at the driver position, as illustrated in Fig. 1b. Journeys were equally distributed between mornings (10-12 am; $J_{1–15}$) and afternoons (16-18 pm; $J_{16–30}$) to observe the daily exposure of passengers to nanoparticles under different traffic conditions.

The length of the chosen route was 2.7 kilometres, connecting the University of Surrey campus with Guildford town centre (Fig 1a), and the speed limit 48 km h^{-1} (30 mph). The

route can be split into three main sub-sections, between the points marked in the figure as A_1 to A_4. Journey times for morning and afternoon trips were 7±2 and 10±3 minutes, respectively, with corresponding average vehicle speeds of 22±4 and 18±3 km h^{-1}. Details of route characteristics and traffic are summarised in Table 2. The experiments were conducted during the winter time, in January and February 2011. Wind, temperature and humidity conditions from the London Heathrow Meteorological Station (approximately 27 km to the north of Guildford) during the experimental periods are summarised in Table 3; note that these indicate neutrally stable boundary layer conditions.

2.2. Instrumentation and data collection

An unleaded petrol-fuelled car (Volkswagen Golf; 1998 registration; 1600cc) was used for the study and a non–smoking driver was the only occupant of the car during the experiments. The air conditioning system was off, all windows closed and the air intake ventilation fan operated at a medium setting (2 on a scale of 1–4) during the experiments. The flow rate provided by the ventilation system (4.2×10^{-2} m^3 s^{-1}) contribute to the total outdoor air exchange rate (7.7×10^{-2} m^3 s^{-1}) in the car cabin, which was estimated by means of tracer gas technique. The remaining is due to air leak through the sealings. The experimental car was not equipped with the filter fitted ventilation system and air conditioning (heating) was kept off during the experiments.

The Cambustion DMS50 was deployed to measure number concentrations and size distributions of particles in the 5–560 nm size range at a sampling rate of 1 Hz, the instrument response time being 500 ms. The instrument was calibrated by the manufacturer (Cambustion Ltd.) in August 2010 and was within the one year calibration validation period. The calibration procedure is described in Cambustion (2007-8).

A short length, 0.50 m, of 5 mm internal diameter, electrically and thermally conductive sampling tube was used to minimise particle losses during sampling (Kumar et al., 2008b). Particle residence times were about 0.3 s at the instrument's sampling flow rate of 6.5 lit min^{-1}. The sample flow rate was maintained by an electrical pump and a classifier restrictor located within the body of the DMS50. The flow rate and zero reading of the instrument were checked prior to each experiment. The DMS50 has a similar operational principle to the DMS500, which has been used extensively in a number of previous studies (e.g. Kumar et al., 2008a, b). The DMS50 is a battery operated, portable version of the DMS500 that is ideal for

on-board measurements (see, e.g. Carpentieri and Kumar, 2011). Details of the operational principal, sensitivity, calibration procedures etc. are available from the Cambustion web-site (Cambustion, 2012). Minimum concentrations measured with the DMS50 on the selected route were found to be well in excess of the instrument signal-to-noise ratio (Cambustion, 2012) at a sampling rate of 1 Hz, the rate used in all the experimental work. The minimum concentrations were basically the background concentrations within the car cabin when there were no other vehicles nearby.

Video recordings were also collected during the experiments using a Canon MVX35 video camera to create a log of emission 'events' ahead of the test vehicle. These were then used to correlate the influence of traffic conditions on measured particle concentrations within the cabin. A GPS tracking system was utilised to log the position and speed throughout each trip. Wind speed and direction were recorded by a local roof top weather station, located as shown in Fig. 1a (see Carpentieri and Kumar, 2011, for further details). The results were broadly consistent with the data shown in Table 3 for the London Heathrow Meteorological Station, which give a better indication of overall conditions.

2.3. Estimation of deposition in the respiratory tract

Nanoparticles in a car cabin are constantly inhaled by the driver and passengers throughout a journey. The total dose received is directly related to the difference between the number of particles inhaled and exhaled during each breath, the breathing rate and the period of exposure (Hofmann, 2011; ICRP, 1994). The inhalation and deposition of particles through the respiratory tract can be estimated in a number of ways, including algebraic and semi-empirical deposition models (Hofmann, 2011). The deposition fraction (DF) model (ICRP, 1994) of the International Commission on Radiological Protection (ICRP) is a commonly accepted approach and is adopted here. We use it to estimate deposition to the respiratory tract as a whole but take two approaches in doing so, as described below.

Tidal volume and breathing rate depend on age, gender and the level of activity (Int Panis et al., 2010; Martin and Finlay, 2007). Here, the typical breathing frequency and tidal volume for a seated adult Caucasian male were applied; i.e. 18 per minute and 0.8 lit, respectively (Hofmann, 2011; ICRP, 1994). Multiplication of the tidal volume and the breathing frequency determines the so-called one minute ventilation (VE). Two standard approaches were applied for calculating the dose rate:

Method (i) used size-dependant DFs and the average size-resolved PNCs for each journey. The size-dependant DFs were taken from the ICRP model (Hofmann, 2011; ICRP, 1994; James et al., 1991).

Method (ii) used a single DF and the average PNC for each journey. This is the usual approach in situations where information on size resolved concentration distributions is not available. A constant DF of 0.65 was assumed, as is widely done in exposure studies for seated subjects (Chalupa et al., 2004; Daigle et al., 2003; Int Panis et al., 2010; Oberdörster et al., 2010).

In each case, the deposition rate of inhaled particles in the respiratory tract was then obtained by multiplying the one minute ventilation by the appropriate DF and journey-averaged particle concentration (Int Panis et al., 2010). Note that the final deposition rate has units of particles per minute.

3. Results and discussion

3.1. PNCs during the journeys and traffic emission events

The results are discussed in terms of the average PNCs during the set of journeys and the individual episodes that were identified by correlating the video images with the measured concentrations. Concentrations are presented in each of the three size ranges 5–30 (N_{5-30}), 30–300 (N_{30-300}) and 300–560 nm ($N_{300-560}$), as well as in total (N_{5-560}). The size range 5–30 nm is taken to define the nucleation mode and 30–300 nm the accumulation mode. As will become apparent below, these two ranges account for over 99% of the total.

3.1.1. Average PNC during journeys

Fig. 2 shows the average PNCs in the car cabin in three size ranges (5–30, 30–300 and 300–560 nm) for each of the 30 trips. Interestingly, the average concentration for all the morning periods, $5.79\pm3.52\times10^4$ cm^{-3}, was similar to that during the afternoons, $5.95\pm4.67\times10^4$ cm^{-3}. Number concentrations were therefore averaged over all journeys for further discussion and comparison with other studies. The result, $5.78\pm4.06\times10^4$ cm^{-3}, was about a factor of two smaller than that recorded in other studies in car cabins but in larger cities, such as Rouen (9.5×10^4 cm^{-3}; Gouriou et al., 2004), London (9.9×10^4 cm^{-3}; Kaur et al., 2004) and Sydney (8.9×10^4 cm^{-3}; Knibbs et al., 2010). It is important to note that the size range extended to 5 nm in our present work, compared with 20 or 30 nm in the other studies (see Table 1), implying that the present results include about 40% of the total concentration in the

5–30 nm size range (see Section 3.1.2) that were not included in the other studies. Adjusted for this, the average PNCs over all journeys reduces to about $3.47 \pm 2.45 \times 10^4$ cm^{-3}. A number of factors could have played a role in generating these differences including: dissimilarities in traffic intensity, differences in the proximity of other vehicles (i.e. sources) to the experimental car, effects of meteorological conditions and presumably higher background concentration compared to Guildford. Mishra et al. (2012) suggest that the variations between different sites could be due to metorological conditions, with the local traffic volume and conditions showing the most dominant effect. They conclude that other dispersion conditions such as; street canyon heights and distance from emission source have profound effect on varations in different site with similar traffic conditions (Mishra et al., 2012).

The ventilation setting in the car cabins could be another important variable (Knibbs et al., 2010) but distinguishing the impacts of these factors on measured PNCs is not straightforward given the available data. The great level of PNCs in the cabin was possibly due to lack of filter fitted ventilation system in the experimental car. Knibbs and de Dear (2010) indicate that filter fitted ventilation systems reduce PNCs in the car cabin significantly. Ventilation system is fitted with outdoor air intake, which could be the possible cause of great level of PNCs in the car cabin. Substantial reduction in PNC levels in the car cabins are reported where ventilation setting were set on indoor air recirculation without outdoor air intake (Knibbs and de Dear, 2010; Fruin et al., 2011; Hudda et al., 2012).

Average concentrations for individual journeys were very variable, with a minimum of 2.42×10^4 cm^{-3} and a maximum of 2.18×10^5 cm^{-3}. The range of 1 s averaged concentrations during individual journeys was even greater; e.g. the minimum and maximum values during journey J_5 were 1.25×10^3 cm^{-3} and 1.85×10^6 cm^{-3}, respectively. This variation in short–term averaged concentrations during a typical journey illustrates the episodic nature of exposure experienced by car commuters. As already noted, the key factors explaining this variability include the distance between the experimental car and preceding vehicles, the type of vehicle ahead (i.e. heavy duty vehicle, bus, diesel or petrol fuelled cars) and the speed of the experimental car, as discussed in detail in Section 3.1.3.

As is clear in Fig. 2, the largest average concentrations were observed during journeys J_5 and J_{19}. In both these cases the test car was close (~1–3 m) to the tailpipe of a heavy duty vehicle and a diesel car, respectively, near to traffic lights where vehicles were moving slowly. The

presence of these vehicles was evident in a sudden burst of fresh particles that led to an increase (1.47×10^5 cm^{-3}) in the proportion of nucleation mode particles (5–30 nm range) by about a factor of 4 relative to the average PNCs in the same size range for all journeys (3.44×10^4 cm^{-3}), see also Section 3.1.3.

3.1.2. Proportion of PNCs in selected size ranges

Average PNCs for all journeys indicated that the fraction of particle numbers in the 300–560 nm range was negligible, both in the mornings and afternoons (see Supplementary Information, SI, Figure S1). In both periods, approximately 55 and 45% were in the 5–30 and 30-300 nm ranges, respectively. These results are consistent with previous measurements that suggest that a large proportion of PNCs emitted by road vehicles are less than 300 nm in diameter (Kittelson, 1998; Knibbs and de Dear, 2010; Zhang and Zhu, 2011). However, the precise proportions might differ slightly from those measured in car cabins in other studies. For instance, Hudda et al. (2011) investigated particle numbers in the size ranges 14–400 nm in a range of vehicles. However, sufficient details of PND data were not available from Hudda et al. (2011) study for direct comparisons.

3.1.3. PNCs during emission episodes

Cabin PNC data were correlated with accompanying video footage in order to investigate the character of number concentrations during episodes of high concentration levels in the car due to emissions from nearby traffic. Such episodes occurred when the test car was idling at traffic lights, moving slowly, or was very close to the tailpipe of a preceding vehicle; e.g. buses, HDVs (e.g. lorries), and diesel or petrol cars. This analysis is particularly interesting, as such correlations have not featured in any detail in previous studies (e.g. Berghmans et al., 2009; Int Panis et al., 2010; Jacobs et al., 2010; Knibbs and de Dear, 2010). As demonstrated by Fig. 3, the correlation analysis indicated short–term increases to values of the order of 10^5 cm^{-3} during "traffic ahead" conditions (defined as conditions when the preceding vehicle was approximately 10 m of the test car based on visual subjective analysis of the video). These peaks can easily be missed while using instruments with poor response times or by representing exposure in terms of the average concentration for a journey (e.g. $5.78\pm4.06\times10^4$ cm^{-3}). Conversely, concentrations were typically of the order 10^3 cm^{-3} (e.g. $7.50\pm5.67\times10^3$ cm^{-3}), which is taken to be equivalent to route background. Comparison of video images obtained during each journey indicated that proximity to the tailpipe of a preceding vehicle was the dominant factor correlated with high particle concentrations,

followed by the traffic volume on the test route. Other factors, including local conditions on the study route, ventilation settings, sampling method and instrument could not be examined as they were fixed during the experiments.

Six journeys: J_{19}, J_5, J_9, J_8, J_2 and J_{26} (see Fig. 3) were selected for further analysis to investigate the behaviour of PNCs and PNDs (see also Section 3.2.2). Each journey lasted for about 430 s and was divided into four distinct events, as illustrated by the temporal evolution of PNCs in Fig. 3. Table 4 summarises the probable causes of each event, E_i to E_{iv}, identified in Fig. 3. Journey 19 (Fig. 3–J_{19}) featured the largest number of particles in the 5-30 nm range of all the journeys undertaken (Fig. 2). The PNC series for J_{19} includes a clear episode, E_{iii}, during which the concentration rapidly increased to a maximum of 1.33×10^6 cm^{-3}, which was about 100 times greater than the lowest level, 1.30×10^4 cm^{-3}, experienced on this journey, or about 6 times greater than the average concentration, $2.18\pm2.99\times10^5$ cm^{-3} (see Fig. 2). During this particular journey, 92% of particles in the measurement range were in the 5–30 nm, leaving only 8% in the 30–300 nm size range, compared with average figures for afternoon journeys of 52% and 48 %, respectively. This finding is entirely consistent with previous studies which indicated that the number of particles smaller than 50 nm contributed up to 90% of the total in diesel exhaust plumes (Kittelson, 1998; Knibbs et al., 2011). This in turn suggests that fresh emissions (i.e. particles in the nucleation mode) were likely to be present in the car cabin under journey conditions such as queuing at traffic lights or travelling in congested traffic. Furthermore, the correlation of the video footage and particle measurements during J_{19} also indicated elevated concentrations in the nucleation mode when the test car was close to a 2010 registration diesel passenger, presumably fitted with a diesel particulate filter. It should be noted that meteorological conditions remained almost consistent during morning and afternoon measurements on each day, see Table 3. This possibly indicates that the meteorological conditions had minimal effects on measurement differences between morning and afternoon.

3.2. Particle size distributions

3.2.1. Averaged PNDs during journeys

Whilst the average PNCs for all morning experiments were almost the same as for the afternoon experiments (see Section 3.1.1, Fig. 2), average PNDs showed distinct differences (Fig. 4). One clear difference was the much greater number of particles in the 5–10 nm size range in the afternoon journeys (Fig 4b) than in the morning (Fig 4a). This may be due to

slightly slower moving traffic during afternoon journeys (i.e. an average of 18 km h^{-1} compared with 22 km h^{-1} in the mornings) leading to somewhat decreased separation between the test car and vehicle ahead and resulting in a greater number of freshly emitted particles entering the cabin.

Average PNDs during each of the six selected journeys are plotted in Fig. 5, the corresponding PNCs are shown in Fig. 3 and journey features are listed in Table 4. Fig. 5–J_{19}, shows a large peak in the 5-10 nm size range as a result of the test car travelling just behind a diesel car, (see J_{19} in Table 4). In fact, the number of particles in this range increased rapidly during emission event E_{iii} (Fig. 3–J_{19}), which dominated average PNDs for the whole journey. On the other hand, Fig. 5–J_5 shows a distinct mode dominated by particles in the 10–40 nm size range. The presence of these larger particles probably reflects poorer dilution conditions (i.e. driving in congested conditions) allowing particles to grow in size due to transformation processes, in particular coagulation (Ketzel and Berkowicz, 2004; Kumar et al., 2011b). The PNDs shown in Fig.5-J_9 and J_8 have similar shapes, with a bi-modal distribution that indicates the presence of significant numbers of nucleation and accumulation mode particles. During journeys J_9 and J_8, PNDs in the 5-30 nm size range showed significant reduction compared to J_{19} and J_5 (Fig. 5). This may be due to higher dilution, which occurred at a relatively steady speed (i.e. 22±4 km h^{-1}), and greater vehicle separation in the absence of congestion.

Fig.5-J_2 and J_{26} also illustrate bi-modal distributions. Review of recorded images of traffic conditions reveals that during these two journeys (J_2 and J_{26}), the traffic conditions followed a similar trend (i.e. in general; very light traffic, moving smoothly with occasional stops). This, once more, highlights the great influence of traffic conditions and proximity to preceding vehicles on PNCs and PNDs in the car cabin.

3.2.2. Particle dynamics during emission episodes

Detailed analysis to investigate the development of the PND and the particle dynamics were carried out for all experimental journeys. Using the recorded video, significant events were identified during each journey. Therefore, each journey was divided into unequal intervals (i.e. denoted sub-domains ‘a’ to ‘h’) to highlight the effect of driving and traffic conditions on PNDs in the car cabin. However, some degrees of repetitiveness were observed between correlation of PNCs in the cabin and traffic conditions, therefore,

only two journeys (J_{19} and J_8) with distinctive road traffic conditions were presented; the other cases are included in SI Section S.3.

Fig. 6 shows the evolution of PNCs during J_{19}. The record is divided into six sub–domains (a–f) and the average PNDs in each sub-domain are plotted in sequence in Fig. 6a–f. The associated traffic conditions are summarised in Table 4. The PND for sub-domain J_{19a}, Fig. 6a, shows no obvious contributions from fresh emissions and can be regarded as a background distribution. In freely flowing traffic, PNCs increase and fresh emission start to be seen in the PNDs as a peak that appears at around 6 nm (see sub-domain J_{19b} in Fig. 6b). Except the first 20 seconds of the journey, PNDs were bi-modal throughout the journey despite; variations of the magnitude of the 6 nm peak.. There is also an associated but relatively small increase in the number of particles that are larger than 10 nm. This process is clearly seen as the test vehicle enters congested conditions, sub-domain J_{19c} (Fig. 6c), and becomes most pronounced when driving close to a diesel car, sub-domain J_{19d} (Fig. 6d). In this example, the number of particles below 10 nm in size reaches about 3×10^6 cm^{-3}, in broad terms an order of magnitude increase relative to preceding conditions (Fig. 6d). Then, as the traffic again becomes free-flowing, both the PNC and the magnitude of the 6 nm peak in the PND decay as 'cleaner' air enters the cabin (Fig. 6e). Sub-domain J_{19f} (Fig. 6f) indicates that away from traffic, the PND curve has similar magnitude to those measured at the background, shown in Fig. 6a. This is essentially a dilution process. This is consistent with previous studies, in which dilution was identified as the dominant and most important process (Carpentieri et al., 2011; Ketzel and Berkowicz, 2004; Kumar et al., 2009a).

Fig. 7 shows the evolution of PNCs during J_8. Again, the record is divided into eight sub-domains (a–h) and the average PNDs for each sub-domain are plotted in sequence in Fig. 7a–h. The associated traffic conditions are summarised in Table 4. The obvious difference between this journey and J_{19} is that the largest PNCs are about a factor of 5 lower. The peak values in J_{19} occurred whilst driving close to a diesel-engine car and that did not happen in J_8. The differences are even more pronounced in the PNDs, with the largest values in J_{19} (sub-domain d) being approximately a factor of twenty larger than any values seen in J_8.

The first sub-domain (Fig. 7a) corresponds to driving behind a petrol car and PND values are even lower than found for the background in J_{19} (sub-domain a). As the test car approached local road works between A_1 and A_2 (see Fig. 1), particle numbers in the accumulation mode

(i.e. D_p >30 nm) increased substantially (Fig. 7b) from the low values in the first domain (Fig. 7a). Traffic movement was slow because of the road works and the distances between vehicles reduced to about 2-3 meters. A steady increase in particle numbers in the nucleation mode (i.e. D_p <30 nm) is observed (Fig. 7b) as a consequence. Traffic moved at higher speeds after the road works and particle numbers in the nucleation mode showed a very slight increase during the acceleration phase. However, numbers in the accumulation mode were steadily reduced by dilution (Fig. 7c). With the increase in traffic speed and greater vehicle separation in the absence of congestion in sub–domain g, nucleation mode particle numbers reduced rapidly from the levels seen in sub–domain c (Fig. 7c) whereas there was only a modest decrease in the numbers of accumulation mode particles (Fig. 7d). A rapid increase of PNCs in both modes was observed during vehicle acceleration in sub-domain e (Fig. 7e), with the increase in the nucleation mode being most pronounced. Except a slight increase to values of particles in nucleation mode in sub–domain g (Fig. 7g), thereafter, dilution dominates and number concentrations and PNDs in the cabin steadily decay during travel in freely flowing traffic in sub–domains f–h (Fig. 7f–h).

As in J_{19}, there were limited changes in the numbers of accumulation mode particles during this journey, even though there were substantial variations in nucleation mode particle numbers. This reflects the longer atmospheric residence time for particles in the accumulation mode compared with those in nucleation mode (Müller, 1984; Seinfeld and Pandis, 2006).

3.3. Respiratory tract deposition

The average dose rates over the 30 journeys using (i) used size-dependant DFs and (ii) constant DF (as described in Section 2.3) were found to be $5.50\pm5.09 \times 10^8$ min^{-1} and $5.41\pm3.62 \times 10^8$ min^{-1}, respectively. Fig. 8 shows that overall the differences (~1.73%) between the estimated doses by the two approaches are trivial. However, some significant differences (up to 30%) were observed (e.g. J_{19}). In general, exposure studies using constant DFs values can provide an adequate approximation of the dose inhaled by commuters. However, an underestimation of dose can be seen for cases in which the vast majority of inhaled particles are in the nucleation mode (i.e. those below 30 nm in diameter).

Dose rates vary substantially from journey to journey, the extremes being about a factor of 4 (during J_{19}) and 2 (during J_5) above the overall average. As expected, comparison of Fig. 2 (total PNCs) and Fig. 8 indicates that the largest doses occur in those journeys where PNC

levels are greatest. Substantial increases in dose rate were identified during traffic conditions (e.g. congestion, preceding diesel vehicle) in which PNCs in the car cabin were dominated by freshly emitted nucleation mode particles.

These estimated dose rates are based on the breathing rate of a healthy average Caucasian male subject in a sitting condition. Estimated dose rates would be different for female subjects (Daigle et al., 2003; Int Panis et al., 2010), children, subjects under exercise (i.e. cycling, etc.) and with different health condition (Chalupa et al., 2004; Donaldson et al., 1998).

Data available for direct comparisons are limited. Int Panis et al. (2010) calculated the dose using a constant DF of 0.63 for a car journey in Brussels (Belgium) and obtained a result of 8.41×10^{5} m^{-1}, which is slightly lower than estimated (i.e. 1.80×10^{6} m^{-1}) for typical journeys in Guildford. The instrument employed (ultrafine particle counter, UPC) in Brussels measures particles in the 20–1000 nm size range, where the cut off size range for the DMS50 employed in this study was 5 nm (see Table 1). Therefore, a factor of two difference is not surprising given all the factors that contribute to the dose estimates. The calculations indicate that the exposure level in the car cabin is very sensitive to traffic composition and conditions along route. The estimates do though demonstrate that the dose calculation with a constant DF and mean PNCs can provide a reasonable approximation to exposure levels. However, size resolved PNDs with corresponding DFs offer a more realistic dose approximation, particularly in extreme cases.

4. Conclusions and future work

The evolution of PNCs and distributions in a car cabin were investigated whilst driving for a total of 30 return journeys on a fixed 2.7 km route in Guildford, UK. A fast response instrument (Cambustion DMS50) was deployed to measure particles in the 5-560 nm size range. The results were then used to calculate the exposure of the driver to nanoparticle pollution on the journeys.

The DMS50 was found to perform satisfactorily in the test environment and its fast response allowed rapid changes in PNCs and distributions to be observed. Averaged number concentrations for the morning and afternoon journeys were effectively the same, the difference being less than 1%. This is somewhat lower than the average values reported for larger cities; e.g. London, Sydney and Rouen. Here, PNC measurements covered particle

443 diameters as small as 5 nm, which enabled measurement of freshly emitted nanoparticles, but
444 the lower cut–off diameters in the other studies were limited to either 10 or 30 nm. However,
445 a number of factors could account for the difference, such as: dissimilarities in traffic
446 intensity, differences in the proximity of other vehicles (i.e. sources) to the test car, effects of
447 meteorological conditions and, presumably, higher background concentrations compared to
448 Guildford (Briggs et al., 2008; Int Panis et al., 2010). Mean PNCs for the 30 trips show
449 variation of up to an order of magnitude. However, the 1 Hz data series demonstrate up to
450 three order of magnitude variations in PNCs during a single journey (e.g. J_5).

451 Video recordings made at the same time as the concentration measurements were used to
452 correlate traffic conditions ahead of the test car with the concentration data. This showed that
453 the dominant factors associated with elevated concentration numbers in the car cabin were
454 the close proximity of the test car to nearby sources (such as heavy duty vehicles, buses,
455 diesel or petrol fuelled cars, particularly in conditions of congested traffic flow) and the speed
456 of the test car.

457 Analysis of PNDs in the car cabin showed that particles in the 5–30 nm and 30–300 nm size
458 ranges contributed approximately 55 and 45% of the total, respectively; the fraction of the
459 total above 300 nm in size was 0.3%. The video records indicated that the high proportion in
460 the 5–30 nm size range resulted from emissions from vehicles travelling slightly ahead of the
461 test car. The evolution of number distributions during each journey showed significant
462 changes in response to events on the road and the emissions they implied. The key factor for
463 high number concentrations in the 5-30 nm range was travelling close to a preceding vehicle
464 in slow moving, congested traffic. The analysis also indicated that dilution was the dominant
465 process affecting particle concentrations in the car cabin. Dilution process acted as a loss
466 mechanism when relatively clean air was drawn into the car, especially in conditions when no
467 traffic was ahead of the experimental car. This process also acted as a gain mechanism,
468 especially when polluted air from outside the car was drawn into the car during the congested
469 traffic conditions.

470 The deposition of particles in the respiratory tract was estimated ($5.50 \pm 5.09 \times 10^8$ min^{-1}) using
471 a size-dependent DF and the average size-resolved PNC. This approach is considered
472 preferable to using a fixed DF and the average PNC, particularly in situations where the
473 distribution changes significantly during the exposure period, though in this case the two

methods yielded almost the same result. The calculated deposition rate was slightly lower than the value reported by Int Panis et al. (2010) for journeys in Brussels.

The nature of on-road measurements and the simultaneous influence of many and varied processes makes it difficult to reach firm conclusions. Exposure rates vary greatly from journey to journey and within any specific journey, in response to local traffic, emission and dispersion conditions, as well as during different seasons (see e.g., Mishra et al., 2012; Fujitani et al., 2012). Thirty journeys is a limited sample from a statistical point of view and insufficient to define typical PNCs in Guildford town centre. However, the trips made provided us enough emission events which were needed to correlate PND variations in the cabin to emission events outside. Future studies should include more precise measurement of the separation between the test and preceding vehicle to determine the sensitivity to this variable. For the same reason, traffic count and composition, and street configuration data should also be included. It will also be useful to develop relationships of size resolved nanoparticle distributions between the inside car cabin and the roadside environments.

5. Acknowledgements

This work is supported by the EPSRC DTA Grant. Thanks also go to a University of Surrey Instrument grant and to Dr. Paul Hayden and Mr. Alistair Reynolds for their help during the experimental campaigns.

6. References

Atkinson, R.W., Fuller, G.W., Anderson, H.R., Harrison, R.M., Armstrong, B., 2010. Urban Ambient Particle Metrics and Health: A Time-series Analysis. Epidemiology 21, 501-511.

Berghmans, P., Bleux, N., Int Panis, L., Mishra, V., Torfs, R., Van, P., 2009. Exposure assessment of a cyclist to PM_{10} and ultrafine particles. Science of the Total Environment 407, 1286 - 1298.

Boogaard, H., Borgman, F., Kamminga, J., Hoek, G., 2009. Exposure to ultrafine and fine particles and noise during cycling and driving in 11 Dutch cities. Atmospheric Environment 43, 4234-4242.

Bos, I., Jacobs, L., Nawrot, T.S., de Geus, B., Torfs, R., Int Panis, L., Degraeuwe, B., Meeusen, R., 2011. No exercise-induced increase in serum BDNF after cycling near a major traffic road. Neuroscience Letters 500, 129-132.

Briggs, D.J., de Hoogh, K., Morris, C., Gulliver, J., 2008. Effects of travel mode on exposures to particulate air pollution. Environment International 34, 12-22.

Burtscher, H., 2001. Literature study on tailpipe particulate emission measurement for diesel engines, Particle Measurement Programme for BUWAL/GRPE.

Buseck, P.R., Adachi, K., 2008. Nanoparticles in the atmosphere. Elements 4, 389-394.

510 Cambustion, 2012. DMS50 Fast Particulate Spectrometer: Introduction and features.
511 www.cambustion.com/products/dms50 (accessed July 2012).
512 Carpentieri, M., Kumar, P., 2011. Ground-fixed and on-board measurements of nanoparticles
513 in the wake of a moving vehicle. Atmospheric Environment 45, 5837-5852.
514 Carpentieri, M., Kumar, P., Robins, A., 2011. An overview of experimental results and
515 dispersion modelling of nanoparticles in the wake of moving vehicles. Environmental
516 Pollution 159, 685-693.
517 Chalupa, D.C., Morrow, P.E., Oberdörster, G., Utell, M.J., Frampton, M.W., 2004. Ultrafine
518 Particle Deposition in Subjects with Asthma. Environmental Health Perspectives 112,
519 879-882.
520 Daigle, C.C., Chalupa, D.C., Gibb, F.R., Morrow, P.E., Oberdörster, G., Utell, M.J.,
521 Frampton, M.W., 2003. Ultrafine Particle Deposition in Humans During Rest and
522 Exercise. Inhalation Toxicology 15, 539-552.
523 Donaldson, K., Li, X., Macnee, W., 1998. Ultrafine (nanometre) particle mediated lung
524 injury. Journal of Aerosol Science 29, 553-560.
525 Donaldson, K., Tran, L., Albert Jimenez, L.A., Duffin, R., Newby, D.E., Mills, N., MacNee,
526 W., Stone, V., 2005. Combustion-derived nanoparticles: A review of their toxicology
527 following inhalation exposure. Particle & Fibre Toxicology 5/6, 553-560.
528 Dons, E., Int Panis, L., Van Poppel, M., Theunis, J., Willems, H., Torfs, R., Wets, G., 2011.
529 Impact of time–activity patterns on personal exposure to black carbon. Atmospheric
530 Environment 45, 3594-3602.
531 Dons, E., Int Panis, L., Van Poppel, M., Theunis, J., Wets, G., 2012. Personal exposure to
532 Black Carbon in transport microenvironments. Atmospheric Environment 55, 392-398.
533 Ghio, A., Kim, C., Devlin, R., 2000. Concentrated ambient air particles induce mild
534 pulmonary inflammation in healthy human volunteers. American Journal of Respiratory
535 and Critical Care Medicine 162, 981-988.
536 Gouriou, F., Morin, J.P., Weill, M.E., 2004. On-road measurements of particle number
537 concentrations and size distributions in urban and tunnel environments. Atmospheric
538 Environment 38, 2831-2840.
539 Guildford-Borough, 2008. State of Guildford Borough report. Guildford-Borough, Guildford.
540 Hofmann, W., 2011. Modelling inhaled particle deposition in the human lung—A review.
541 Journal of Aerosol Science 42, 693-724.
542 Hudda, N., Kostenidou, E., Sioutas, C., Delfino, R.J., Fruin, S.A., 2011. Vehicle and driving
543 characteristics that influence in-cabin particle number concentrations. Environmental
544 Science & Technology 45, 8691-8697.
545 ICRP, 1994. Human Respiratory Tract Model for Radiological Protection. ICRP Publication
546 66, 1-3.
547 Int Panis, L., de Geus, B., Vandenbulcke, G., Willems, H., Degraeuwe, B., Bleux, N., Mishra,
548 V., Thomas, I., Meeusen, R., 2010. Exposure to particulate matter in traffic: A
549 comparison of cyclists and car passengers. Atmospheric Environment 44, 2263-2270.
550 Jacobs, L., Nawrot, T., de Geus, B., Meeusen, R., Degraeuwe, B., Bernard, A., Sughis, M.,
551 Nemery, B., Panis, L., 2010. Subclinical responses in healthy cyclists briefly exposed to
552 traffic-related air pollution: an intervention study. Environmental Health 9, 64.
553 James, A.C., Stahlhofen, W., Rudolf, G., Egan, M.J., Nixon, W., Gehr, P., Briant, J.K., 1991.
554 The Respiratory Tract Deposition Model Proposed by the ICRP Task Group. Radiation
555 Protection Dosimetry 38, 159-165.
556 Kasper, M., 2005. Sampling and measurement of nanoparticle emissions for type approval
557 and field control. SAE Technical Paper Series. Society of Automobile Engineers 26.

Kaur, S., Clark, R.D.R., Walsh, P.T., Arnold, S.J., Colvile, R.N., Nieuwenhuijsen, M.J., 2006. Exposure visualisation of ultrafine particle counts in a transport microenvironment. Atmospheric Environment 40, 386-398.

Kaur, S., Nieuwenhuijsen, M., Colvile, R., 2005. Personal exposure of street canyon intersection users to PM2.5, ultrafine particle counts and carbon monoxide in Central London, UK. Atmospheric Environment 39, 3629-3641.

Kaur, S., Nieuwenhuijsen, M.J., Colvile, R.N., 2007. Fine particulate matter and carbon monoxide exposure concentrations in urban street transport microenvironments. Atmospheric Environment 41, 4781-4810.

Ketzel, M., Berkowicz, R., 2004. Modelling the fate of ultrafine particles from exhaust pipe to rural background: an analysis of time scales for dilution, coagulation and deposition. Atmospheric Environment 38, 2639-2652.

Kittelson, D.B., 1998. Engines and nanoparticles: a review. Journal of Aerosol Science 29, 575-588.

Knibbs, L.D., Cole-Hunter, T., Morawska, L., 2011. A review of commuter exposure to ultrafine particles and its health effects. Atmospheric Environment 45, 2611-2622.

Knibbs, L.D., de Dear, R.J., 2010. Exposure to ultrafine particles and PM2.5 in four Sydney transport modes. Atmospheric Environment 44, 3224-3227.

Knibbs, L.D., de Dear, R.J., Morawska, L., 2010. Effect of Cabin Ventilation Rate on Ultrafine Particle Exposure Inside Automobiles. Environmental Science & Technology 44, 3546-3551.

Kumar, P., Fennell, P., Langley, D., Britter, R., 2008a. Pseudo-simultaneous measurements for the vertical variation of coarse, fine and ultrafine particles in an urban street canyon. Atmospheric Environment 42, 4304-4319.

Kumar, P., Fennell, P., Symonds, J., Britter, R., 2008b. Treatment of losses of ultrafine aerosol particles in long sampling tubes during ambient measurements. Atmospheric Environment 42, 8819-8826.

Kumar, P., Robins, A., Britter, R., 2009a. Fast response measurements of the dispersion of nanoparticles in a vehicle wake and a street canyon. Atmospheric Environment 43, 6110-6118.

Kumar, P., Robins, A., Vardoulakis, S., Britter, R., 2010. A review of the characteristics of nanoparticles in the urban atmosphere and the prospects for developing regulatory controls. Atmospheric Environment 44, 5035-5052.

Kumar, P., Gurjar, B.R., Nagpure, A., Harrison, R.M., 2011a. Preliminary estimates of nanoparticle number emissions from road vehicles in megacity Delhi and associated health impacts. Environmental Science and Technology 45, 5514-5521.

Kumar, P., Ketzel, M., Vardoulakis, S., Pirjola, L., Britter, R., 2011b. Dynamics and dispersion modelling of nanoparticles from road traffic in the urban atmospheric environment - a review. Journal of Aerosol Science 42, 580-603.

Martin, A.R., Finlay, W.H., 2007. A general, algebraic equation for predicting total respiratory tract deposition of micrometer-sized aerosol particles in humans. Journal of Aerosol Science 38, 246-253.

Mishra, V.K., Kumar, P., Van Poppel, M., Bleux, N., Frijns, E., Reggente, M., Berghmans, P., Int Panis, L., Samson, R., 2012. Wintertime spatio-temporal variation of ultrafine particles in a Belgian city. Science of the Total Environment 431, 307-313.

Morawska, L., Ristovski, Z., Jayaratne, E.R., Keogh, D.U., Ling, X., 2008. Ambient nano and ultrafine particles from motor vehicle emissions: Characteristics, ambient processing and implications on human exposure. Atmospheric Environment 42, 8113-8138.

607 Müller, J., 1984. Atmospheric residence time of carbonaceous particles and particulate pah-
608 compounds. Science of the Total Environment 36, 339-346.
609 Oberdorster, G., 2000. Toxicology of ultrafine particles: in vivo studies. Philosophical
610 Transactions of the Royal Society of London A 358, 2719-2740.
611 Oberdörster, G., Elder, A., Finkelstein, J., Frampton, M., Hopke, P., Peters, A., Prather, K.,
612 Wichmann, E., Utell, M., 2010. Assessment of ambient UFP health effects: Linking
613 sources to exposure and responses in extrapulmonary organs, Environmental Protection
614 Agency. University of Rochester, Rochester, p. 35.
615 Paatero, P., Aalto, P., Picciotto, S., Bellander, T., Castano, G., Cattani, G., Cyrys, J., Koster,
616 M., 2005. Estimating time series of aerosol particle number concentrations in the five
617 HEAPSS cities on the basis of measured air pollution and meteorological variables.
618 Atmos. Environ. 39, 2261-2273.
619 Peters, A., von Klot, S., Heier, M., Trentinaglia I., Hormann A., Wichmann, H.E., Lowel, H.
620 2004. Exposure to traffic and the onset of myocardial infarction. New England Journal
621 of Medicine 351, 1721-1730.
622 Pope, C.A., Ezzati, M., Dockery, D.W., 2009. Fine-Particulate Air Pollution and Life
623 Expectancy in the United States. New England Journal of Medicine 360, 376-386.
624 Rim, D., Siegel, J., Spinhirne, J., Webb, A., McDonald-Buller, E., 2008. Characteristics of
625 cabin air quality in school buses in Central Texas. Atmospheric Environment 42, 6453-
626 6464.
627 Seinfeld, J.H., Pandis, S.N., 2006. Atmospheric Chemistry and Physics - From Air Pollution
628 to Climate Change (2nd Edition). John Wiley & Sons.
629 von Klot, S., Cyrys, J., Hoek, G., Kühnel, B., Pitz, M., Kuhn, U., Kuch, B., Meisinger, C.,
630 Hörmann, A., Wichmann, H.E., Peters, A., 2011. Estimated Personal Soot Exposure Is
631 Associated With Acute Myocardial Infarction Onset in a Case-Crossover Study.
632 Progress in Cardiovascular Diseases 53, 361-368.
633 Wang, X., Oliver Gao, H., 2011. Exposure to fine particle mass and number concentrations in
634 urban transportation environments of New York City. Transportation Research Part D:
635 Transport and Environment 16, 1361-9209.
636 Wichmann, H.-E., Peters, A., 2000. Epidemiological evidence of the effects of ultrafine
637 particle exposure. Philosophical Transactions of the Royal Society of London. Series A:
638 Mathematical, Physical and Engineering Sciences 358, 2751-2769.
639 Fujitani, Y., Kumar, P., Tamura, K., Fushimi, A., Hasegawa, S., Takahashi, K., Tanabe, K.,
640 Kobayashi, S., Hirano, S., 2012. Seasonal differences of the atmospheric particle size
641 distribution in a metropolitan area in Japan. Science of the Total Environment 437, 339-
642 347.
643 Zhang, Q., Zhu, Y., 2011. Performance of School Bus Retrofit Systems: Ultrafine Particles
644 and Other Vehicular Pollutants. Environmental Science & Technology 45, 6475-6482.
645 Zhu, Y., Eiguren-Fernandez, A., Hinds, W.C., Miguel, A.H., 2007. In-cabin commuter
646 exposure to ultrafine particles on Los Angeles freeways. Environmental Science and
647 Technology 41, 2138-2145.

Figure captions

Fig. 1. (a) An overview of the study route from A1 to A4; points A1-A4 on the map mark journey segments described in Table 2; location of local weather station marked by diamond point; (b) Schematic diagram of the test car showing DMS50 mounted on rear seat, 11 (v) battery; the sampling point and sampling tube is shown by a white line.

Fig. 2. Average particle number concentrations in three size ranges (5-30, 30-300, 300-560 nm) during each journey; (a) morning (b) afternoon. For sake of clarity, only the positive standard deviation bars are included.

Fig. 3. PNC variations during journeys J_{19}, J_5, J_9, J_8, J_2, and J_{26}. Four significant road events during each journey are marked as E_i, E_{ii}, E_{iii} and E_{iv}.

Fig. 4. Average particle number distributions for all journeys during (a) morning and (b) afternoon. For sake of clarity, only the positive standard deviation bars are included.

Fig. 5. Average particle number distributions for six journeys J_{19}, J_5, J_9, J_8, J_2, and J_{26}. For sake of clarity, only the positive standard deviation bars are included.

Fig. 6. Particle number distributions in selected periods (a-j) of Journey 19. The periods are defined in the top figure, which shows the 1Hz particle number concentrations throughout the journey.

Fig. 7. Particle number distributions in selected periods (a-j) of Journey 5. The periods are defined in the top figure, which shows the 1Hz particle number concentrations throughout the journey.

Fig. 8. Respiratory tract deposition dose rate (# min^{-1}) calculated using (i) size dependent DFs and average size resolved PNCs and (ii) a constant DF and the average PNC for each journey.

List of Tables

Table 1: Summary of recent studies of PNCs in transport modes. A rate of 1 Hz was used in all cases quoted.

Source	**Location**	**Instrument (model)**	**Size range (nm)**	**Transport mode**	**PNC ($\times 10^4$ cm^{-3})**	**Standard deviation ($\times 10^4$ cm^{-3})**
Gouriou et al. (2004)	Rouen (France)	ELPI	30 -1000	Car	9.5	--
Kaur et al. (2005)	London (UK)	UPC- (PTRAK TSI 8525)	20 -1000	Car foot Bus Taxi Cycle	9.9 6.7 10.1 8.7 9.3	1.4 1.4 1.3 1.4 1.4
Zhu et al. (2007)	Los Angeles freeways (USA)	CPC (TSI-3080)	7 - 217	Car	2.5	6.6
Boogaard et al. (2009)	Maastricht (Netherlands)	CPC (TSI-3007)	20 -1000	Car Cycle	3.5 2.8	2 1.7
Jacobs et al. (2010)	Antwerp (Belgium)	UPC (P-TRAK)	20 -1000	Cycle	2.8	0.85
Knibbs and de Dear (2010)	Sydney (Australia)	CPC (TSI-3007)	20 -1000	Train Bus Car Ferry	4.6 10.5 8.9 5.5	-- -- -- --
Int Panis et al. (2010)	Brussels (Belgium)	UPC (P-TRAK)	20 -1000	Car Cycle	2.9 3.5	1.6 1.8
Wang and Oliver Gao (2011)	New York (USA)	CPC (TSI-3785)	5 -3000	Car Metro walk	4.7 1.7 6.06	3.3 0.76 4.4
Hudda et al. (2011)	Pasadena (USA)	CPC (TSI-3007)	10 -1000	car	1.6	--
This Study	Guildford (UK)	DMS50	5 - 560	Car	5.87	3.86

Note: ELPI = Electrical low pressure impactor; UPC = Ultrafine particle counter; CPC = Condensation particle counter; DMS = Differential Mobility Spectrometer

Table 2: Road characteristics and typical traffic conditions for afternoon and morning hours

Route segment	**Road condition**	**Traffic conditions**	
		Morning	**Afternoon**
A1-A2	One lane each way. No traffic light controls. Connects starting point to main routes into the town centre.	Typically no congestion. Outside of rush hour.	Slight congestion around "*Railway Station pick up point*", marked on Fig. 1.
A2-A3	Three lane, one-way road, then three lanes each way. 4 traffic light controls. Roundabouts at each end of segment. Main route into centre; also through route.	Queues at roundabout and traffic lights. Deceleration and acceleration from queues. Slight congestion.	Commonly severe congestion and slow moving traffic.
A3-A4	Single lane, one-way. 1 traffic light control. Access road to town, shopping area and parking centres.	Commonly slow moving traffic with frequent acceleration and deceleration.	Commonly slow moving traffic with frequent acceleration and deceleration.

673
674

Table 3: Meteorological conditions from the London Heathrow Meteorological Station for the experimental periods.

Date	**Time**	**Mean wind speed (ms^{-1})**	**Mean wind direction (degrees)**	**Mean temperature (°C)**	**Mean cloud cover (oktas)**	**Mean relative humidity (%)**
28/01/2011	0800–1200	5.6	60	1.2	7.5	57
	1300–1700	5.4	53	1.4	7.5	57
18/02/2011	0800–1200	3.6	115	6.3	7.3	84
	1300–1700	5.1	125	6.4	6.8	79

675

Table 4. Description of the four emission events identified during each of six journeys J_{19}, J_5, J_9, J_8, J_2, and J_{26} identified in Fig. 3. Events i, ii, iii and iv are defined in the figure.

Journey number	**Event number, see Fig. 3**			
	E_i	E_{ii}	E_{iii}	E_{iv}
J_{19}	Fast moving traffic	Entering congested zone; driving behind diesel car	Behind diesel car	Fast moving traffic
J_5	Slow moving light traffic	Behind a HDV	Behind a HDV in congested traffic	Behind a petrol car
J_9	Passing bus station in town centre	Acceleration from idle behind petrol car	Behind a bus	Background conditions
J_8	Behind a petrol car	Passing road works (excavation)	Waiting at traffic lights	Congested road in town centre
J_2	Passing bus station in town centre	Acceleration from idle behind diesel van	Behind a bus	Passing bus moving in opposite direction
J_{26}	Background conditions	Slow moving traffic	Behind a petrol car	No traffic ahead

676

Figure 1 (Colour)

a

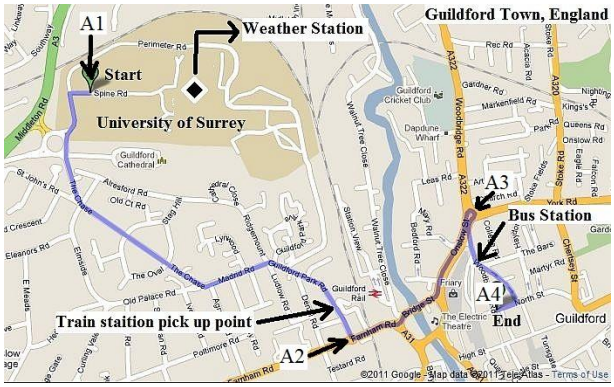

b

Figure 2 (Colour)

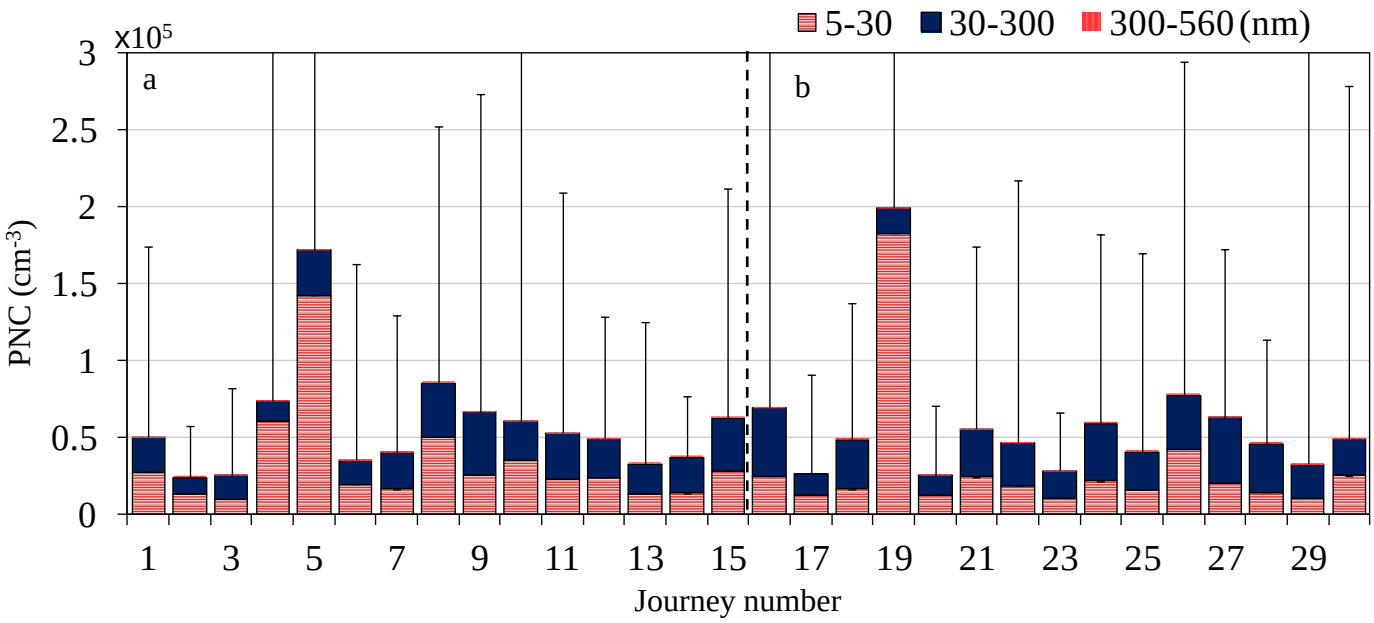

Figure 3 (Colour)

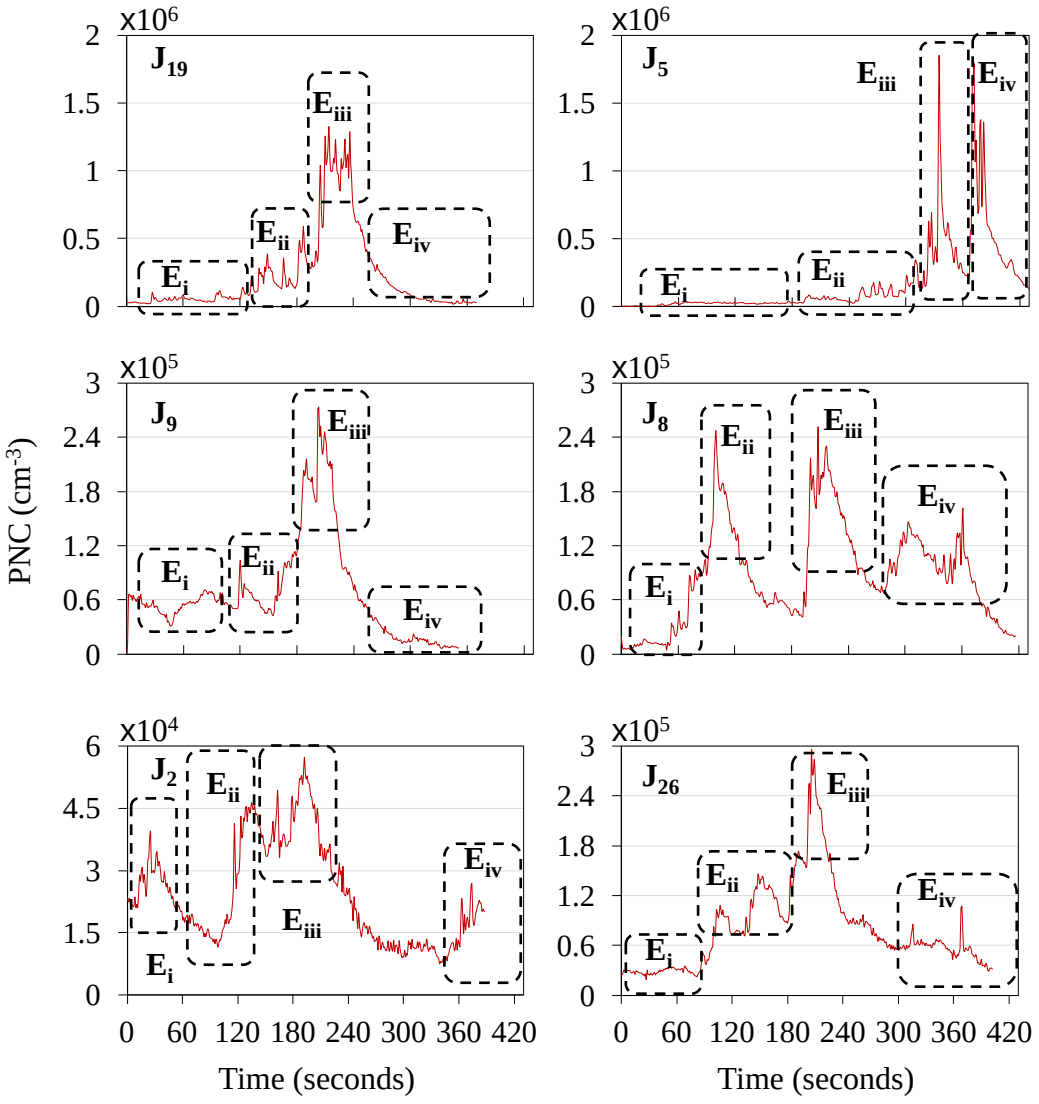

Figure 4 (Colour)

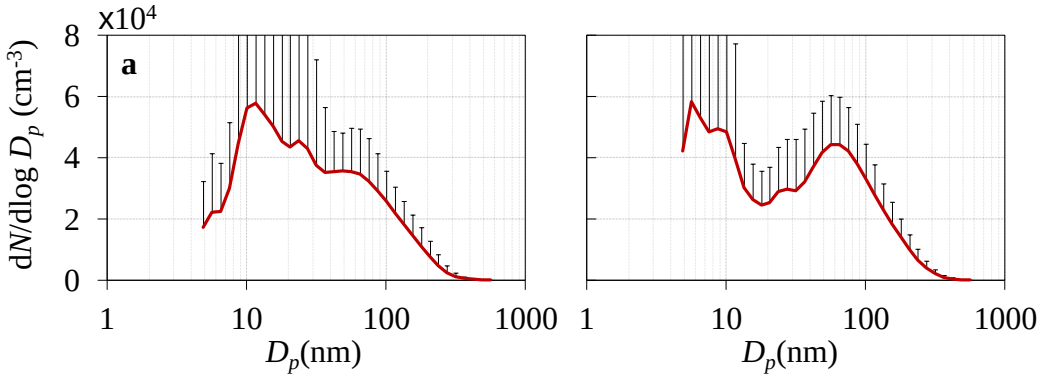

Figure 5 (Colour)

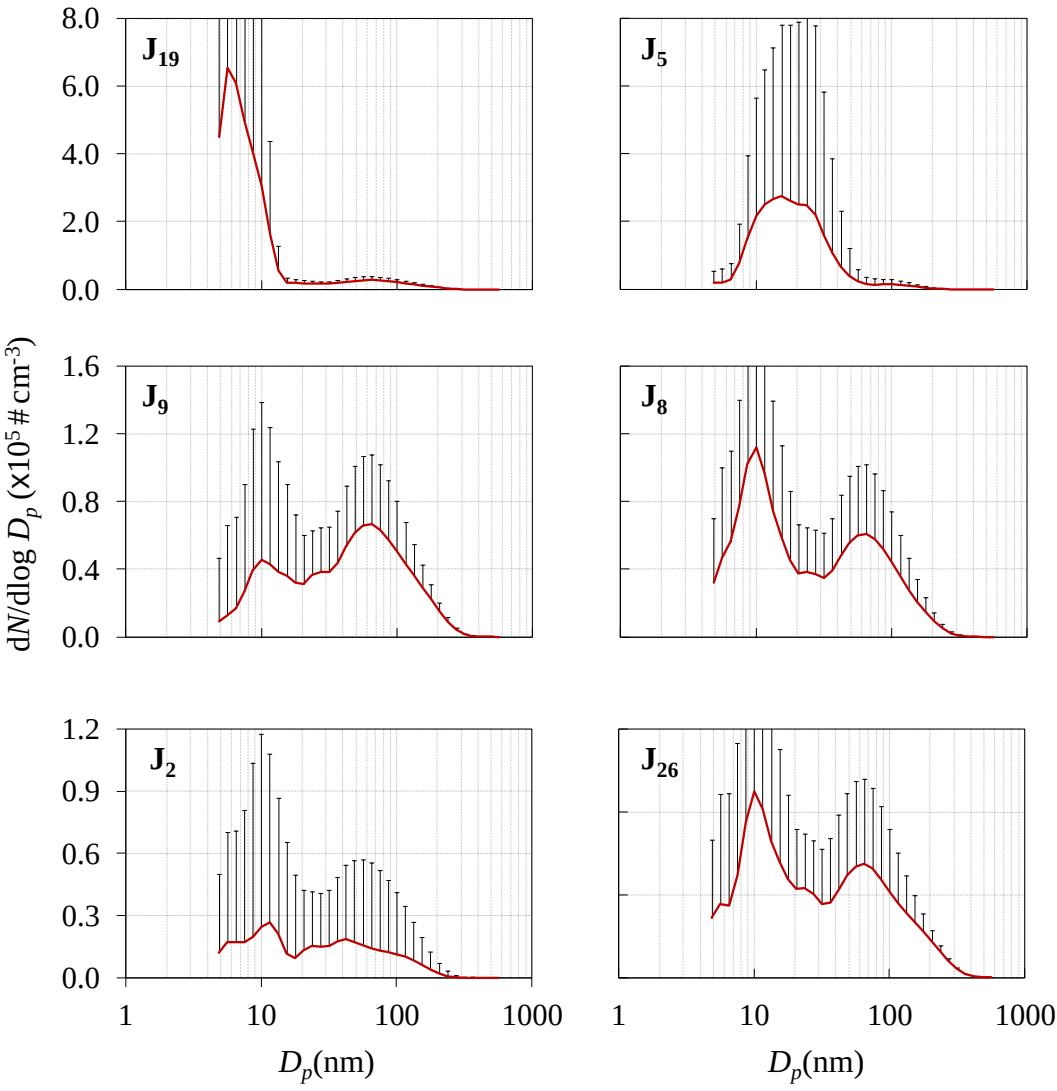

Figure 6 (Colour)

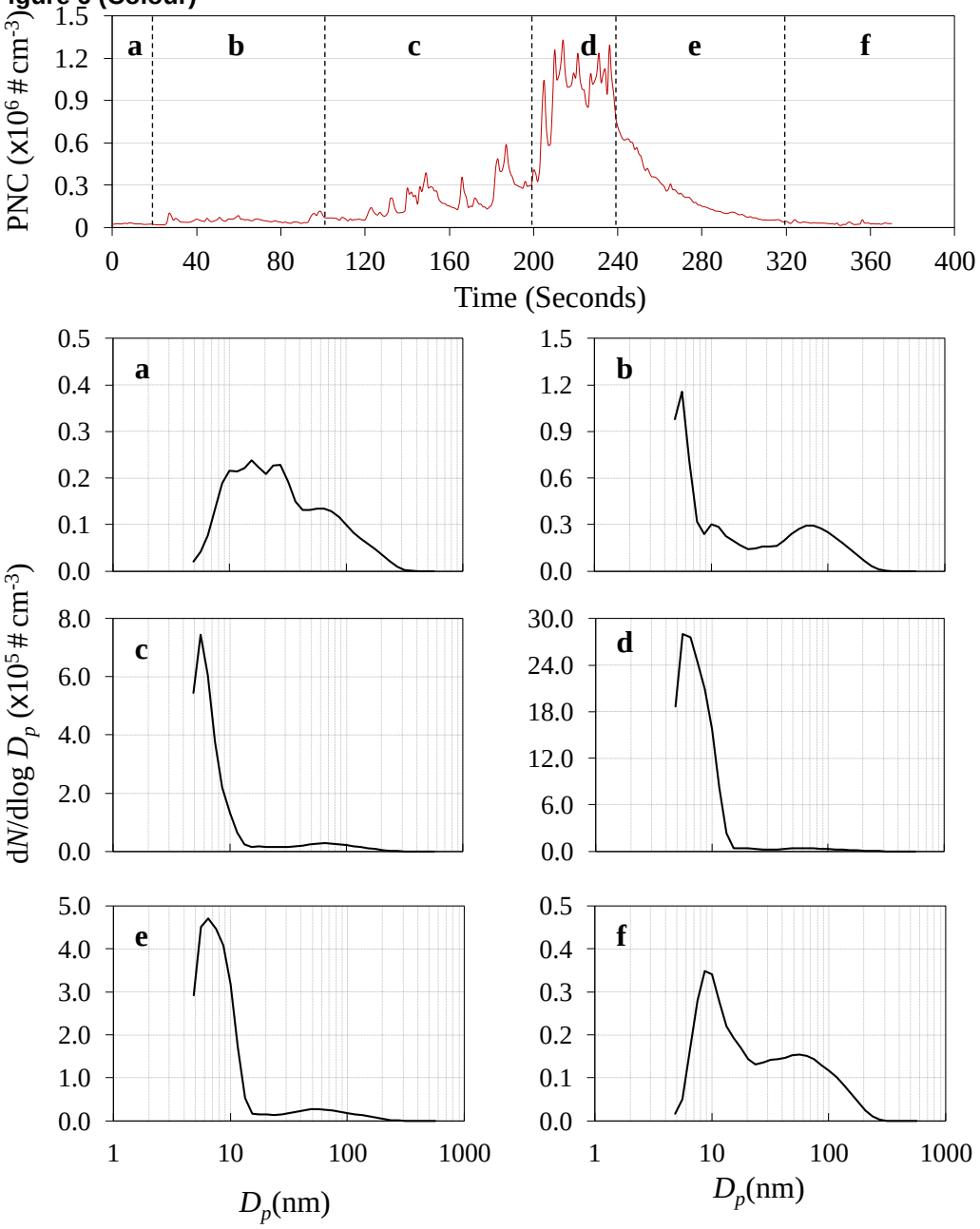

Figure 7 (Colour)

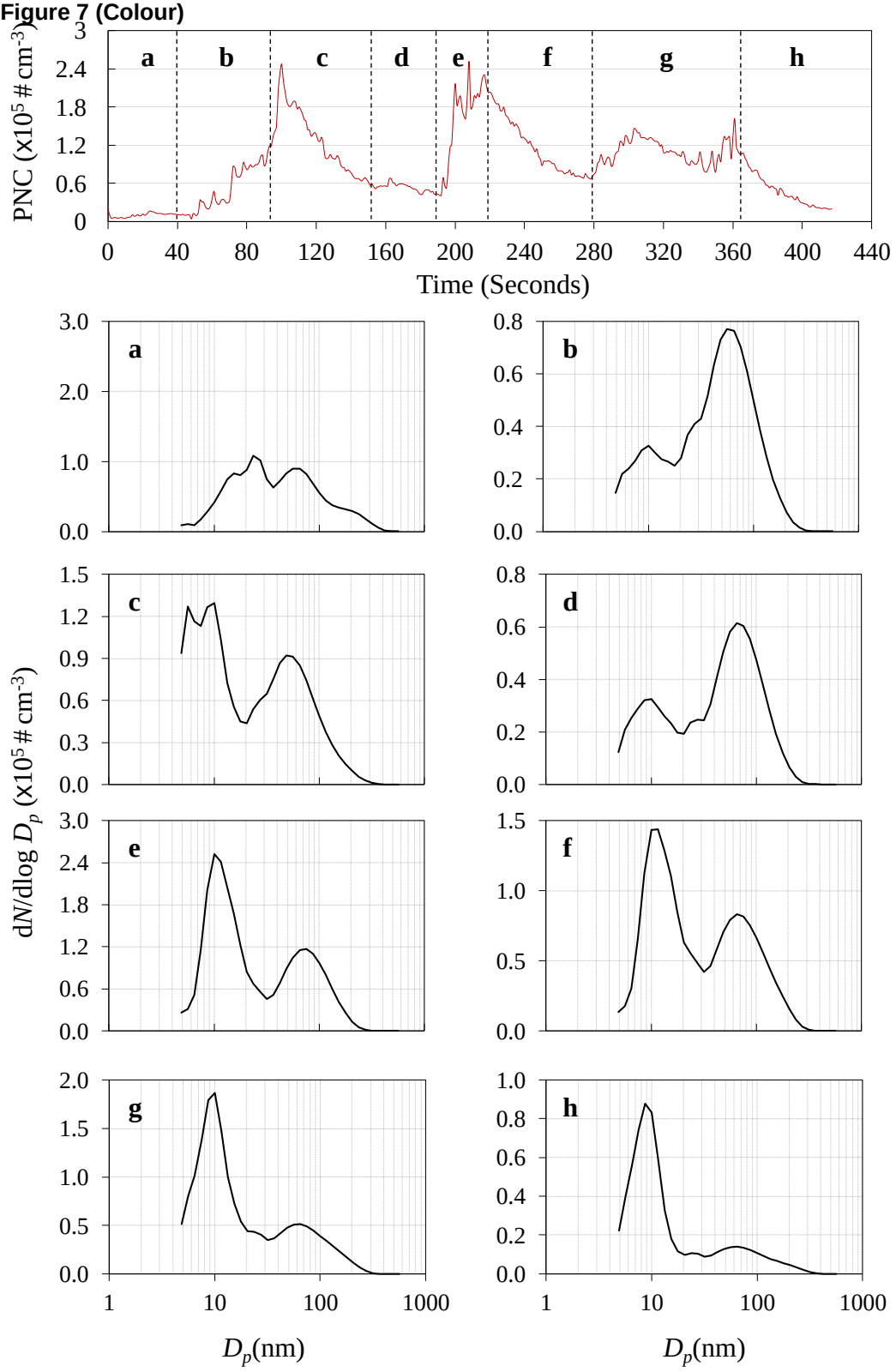

Figure 8 (Colour)

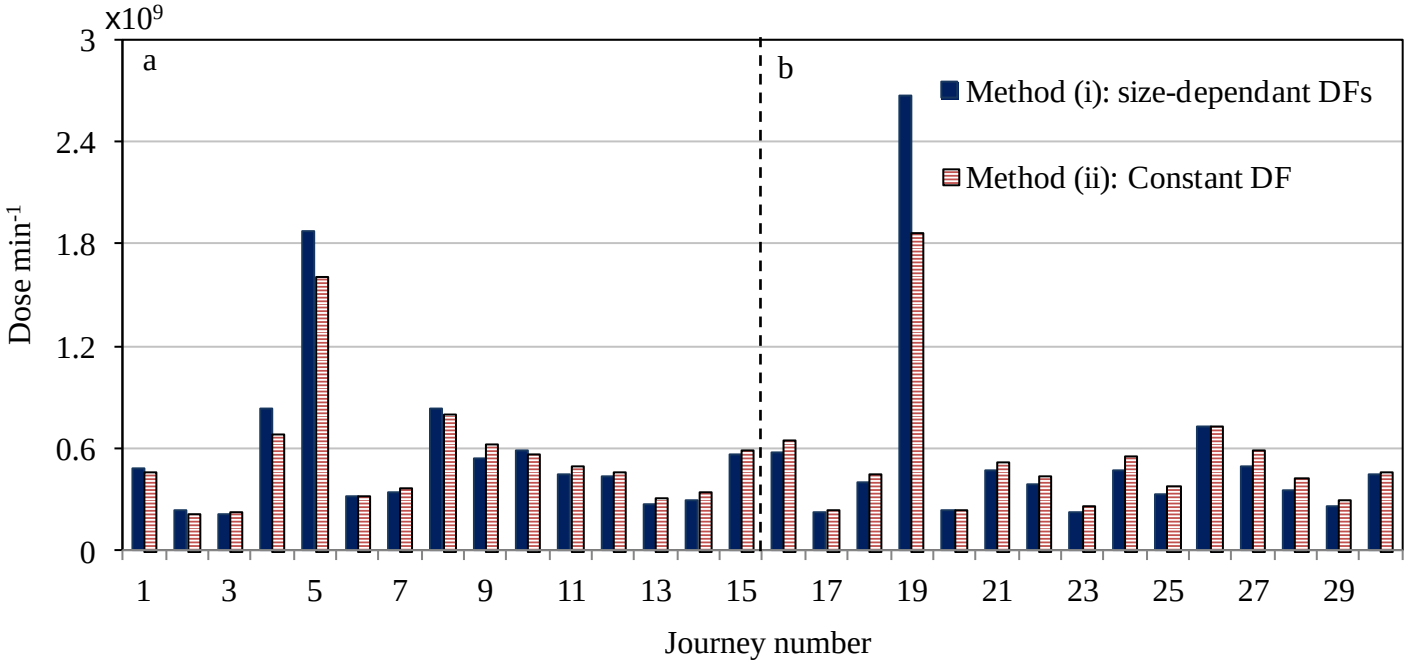

Citation details:
Joodatnia, P., Kumar, P., Robins, A., 2013. The behaviour of traffic produced nanoparticles in a car cabin and resulting exposure rates. Atmospheric Environment 65, 40-51.